HYDROPNEUMATIC SEMI-ACTIVE SUSPENSION SYSTEM WITH CONTINUOUSLY VARIABLE DAMPING

A. Gerhard Vosloo[a], P. Schalk Els[a,*]

[a]Vehicle Dynamics Group, Dept. of Mechanical and Aeronautical Engineering, University of Pretoria, Private Bag x20, Hatfield, 0028, South Africa

*Corresponding author.

E-mail addresses: u12206068@tuks.co.za (A. Gerhard Vosloo), schalk.els@up.ac.za (P. Schalk Els)

Abstract: A hydropneumatic semi-active suspension system for and off-road vehicle, that can switch between two discrete damping characteristics as well as two discrete spring characteristics, has been successfully developed and implemented previously. This paper investigates the feasibility of expanding the concept to include four discrete spring characteristics as well as continuously variable damping by controlling two proportional solenoid valves, which can variably restrict flow paths to two accumulators.

Spring, damping and response time characteristics are determined experimentally, modelled mathematically and validated with experimental measurements. The model incorporates an iterative solver to determine the flow rate through each valve and the change in the accumulator volumes. The accumulator model uses real gas theory, while also taking compressibility of the oil and heat transfer into account. Damping is calculated by a velocity and solenoid current dependant curve-fit model, parameterised from experimental data.

Keywords: semi-active suspension, hydropneumatic, continuously variable damping, accumulator, model, flow split, real gas model

Biographical notes: Gerhard Vosloo is a Master's Degree student in the Vehicle Dynamics Group at the University of Pretoria. His research focus is on the development, characterisation and modelling of a semi-active hydropneumatic spring-damper system with continuously variable damping and four discrete spring characteristics.

Schalk Els is a Professor in Mechanical Engineering at the University of Pretoria and leader of the Vehicle Dynamics Group. His research efforts are focused on improving ride comfort, handling, rollover propensity and life of off-road and heavy vehicles. This includes the use of controllable suspensions systems as well as testing and modelling of large and off-road tyres over rough terrain.

1. INTRODUCTION

A well-known challenge in vehicle dynamics is to design a suspension system that isolates the passengers from road disturbances to provide ride comfort, but also provide handling or road-holding that allows the vehicle to be controlled in a safe and stable manner by the driver. However, the design of a vehicle's suspension system always involves a compromise between these two functions (Els, 2006). Designing for handling requires a stiffer suspension system with low suspension travel, combined with a low vehicle body centre of gravity. On the other hand, designing for ride comfort requires a compliant, soft suspension system with more suspension travel that will be able to absorb the road disturbances. Sport utility vehicles and off-road vehicles are most susceptible to the negative effects of ride comfort orientated suspension characteristics, because they are expected to travel at highway speeds, but also regain off-road mobility where they will experience much rougher roads requiring more suspension travel and ground clearance.

Passive suspension systems have fixed spring and damping characteristics which cannot be changed during operation. A passive suspension system is therefore not capable of achieving the desired combination of good handling and ride comfort as the designer invariably has to make a trade-off by sacrificing one or the other. However, advancements in suspension hardware and control have led to the development of controllable suspensions which can rapidly change their damping and/or spring characteristics during operation. Controllable suspensions combined with a suitable control strategy could therefore reduce or negate the ride comfort and handling compromise by continuously changing the suspension characteristics according to the varying road surfaces or dynamic state of the vehicle.

The proposed controllable suspension that forms the topic of this study, is a newly developed prototype originating from the hydropneumatic 4-state semi-active suspension system, 4S4 (Els, 2006). Els (2006) developed the hydropneumatic 4-state semi-active suspension system, $4S_4$, with the intent of solving this compromise on a Land Rover Defender 110. It is capable of up to four states comprising of two spring and two damping characteristics which are tailored for either ride comfort or handling. The $4S_4$ design, as shown in Figure 1, consists of two pressurised accumulators (with floating pistons), with two state (open or closed) solenoid spool valves that can block or open certain flow paths. With valve 3 open, both gas volumes are compressed, which yields a soft spring characteristic, while when closed, only accumulator 1 is compressed resulting in a high spring characteristic. The damping is controlled by having bypass solenoid valves (valves 1 and 2) for each damper leading to the accumulators. With the bypass valves open, low damping is achieved, while when closed, the fluid is forced through the damper packs resulting in high damping.

A mathematical model of the suspension was developed and experimentally validated (Theron and Els, 2007). This model was used to conduct full vehicle simulations using Adams/Simulink co-simulation platforms. Based on simulations and vehicle implemented test results Els (2006) concluded that the $4S_4$, combined with a suitable control strategy, could successfully reduce the ride comfort and handling compromise on a Land Rover Defender 110.

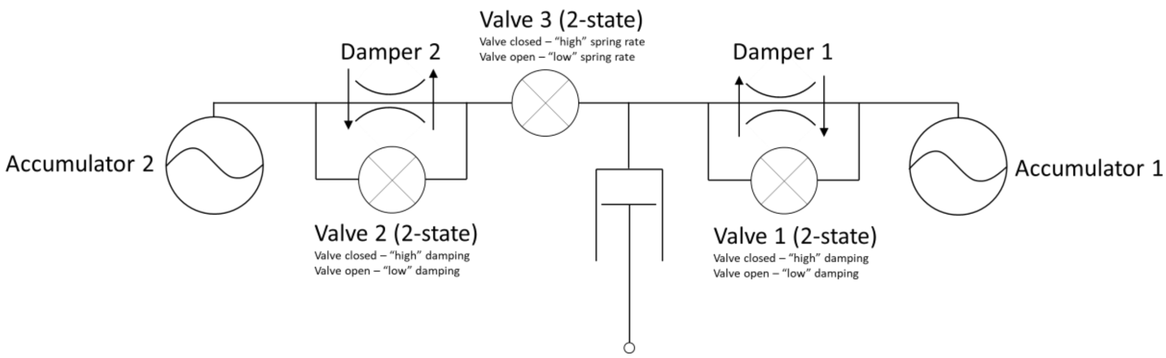

Figure 1: $4S_4$ Design layout (Els, 2006)

In an attempt to improve the successfully implemented $4S_4$, continuously variable damping is incorporated in the suspension system that forms the topic of this study. The newly designed $4S_4$ with continuously variable damping ($4S_4$CVD) is shown in Figure 2 (left). The bypass valves, damper packs and shut-off valves in the previous $4S_4$ are essentially replaced by two solenoid flow-control valves. These valves are responsible to variably restrict flow for increased damping, or blocking flow to decrease the compressible volume for a higher spring characteristic. The $4S_4$CVD is therefore capable of producing any damping characteristic higher than the inherent lower limit with up to four discrete spring characteristics.

The valves selected for the design are electrically variable, pressure-compensated flow-control, spool valves (Hydraforce, 2013). For safety and efficiency, valve V2 is normally closed (NC), while valve V1 is normally open (NO). If the control system should fail, the suspension would therefore revert to a passive, one-accumulator pneumatic spring that would be stiffer and favour handling rather than ride comfort. A 0 to 1.5A current supply is required to control the allowed flow and vary the damping. For the NO valve, 0A would provide minimal damping and maximum damping (flow blocking) at 1.5A and vice versa for the NC valve. For the purposes of this study, only valve V2's cavity was machined, reducing the design layout to the testing layout shown in Figure 2 (right). The suspension fluid could therefore only flow between accumulator 2 and the suspension strut, while flow to accumulator 1 was physically blocked. This was done to reduce the complexity and variables by having only one valve to characterise and model at a time.

Els (2006) also concluded that the $4S_4$ ride comfort performance can further be improved if the lower damping limit and friction is decreased. The $4S_4$CVD design addresses this by reducing the piston diameter from 50mm to 32mm. This reduces flow rate and reduces the low damping limit with the added benefit of reducing the overall package size as smaller accumulators can be used. Furthermore, the floating piston design is replaced with rolling diaphragms, which could reduce the friction and thus make the suspension system more responsive to smaller disturbances. The accumulators can be charged through a non-return valve with nitrogen gas. Nitrogen is used in the pneumatic spring gas as it is an inert gas which is fairly inexpensive and reduces the variables in the system, unlike using atmospheric air, it is a controlled substance. The suspension fluid or oil used is Shell Tellus S2V46 due to its availability and stability across the range of operation. The design allows for fluid pressure measurements before and after each valve, as well as measurement of the gas pressure in the accumulators. The $4S_4$CVD use spherical bearings on the strut and piston rod to allow the suspension to swivel, the output force would therefore be only in the axial direction with negligible moments that could add considerable friction or cause damage.

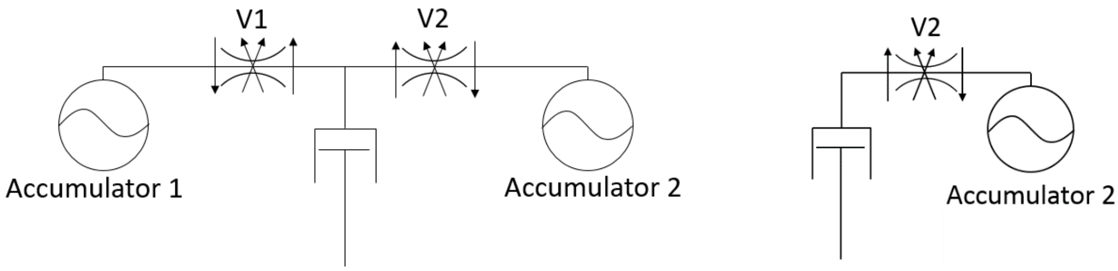

Figure 2: $4S_4$CVD layout
Full design layout (left); manufactured and testing layout (right)

Ultimately, the aim of the $4S_4$CVD is to improve the ride comfort and handling performance of a Land Rover Defender 110 currently equipped with the $4S_4$. To investigate the performance and determine how the $4S_4$CVD should be controlled for improved ride comfort and handling requires an experimentally validated model of the suspension. The purpose of this study was therefore to characterise and model the newly developed $4S_4$CVD, incorporating the pneumatic spring, damping, friction and response time characteristics. This can be used in future research initiatives to conduct vehicle dynamic simulations which incorporate the suspension system.

2. EXPERIMENTAL SETUP

To accurately characterise the $4S_4$CVD, it is mounted to a rigid support frame fitted on top of a 25kN Schenck hydropulse actuator (see Figure 3). The top mounting of the $4S_4$CVD was fixed to the support frame, while the bottom mounting was fixed to the actuator piston via a load cell to measure and record the force output. The various displacement inputs were provided by the actuator, which vertically translated the bottom mounting and piston rod while the rest of the system was fixed to the frame. The actuator has an internal linear variable differential transformer (LVDT), which is used to measure the actuator displacement or suspension deflection. Three pressure transducers were used; one to measure the accumulator gas pressure and the others to measure fluid pressure before and after the valve.

The $4S_4CVD$ was filled with 190ml of oil and the accumulator charged to 7MPa. The charge pressure was selected based on what pressure would be required to support the static and dynamic weight of a Land Rover Defender test vehicle it is ultimately intended for. Care was taken to limit the amount air in the suspension system, however, air diffused in the oil and trapped behind seals are unavoidable and influences the bulk modulus of the oil.

The experimental setup therefore consisted of recording six analogue input channels and controlling two output channels sampled at 1kHz. The six inputs are measurements from three pressure transducers, solenoid current, actuator force and displacement. The two output signals control the actuator (through servo valve controller) and the valve (through current driver).

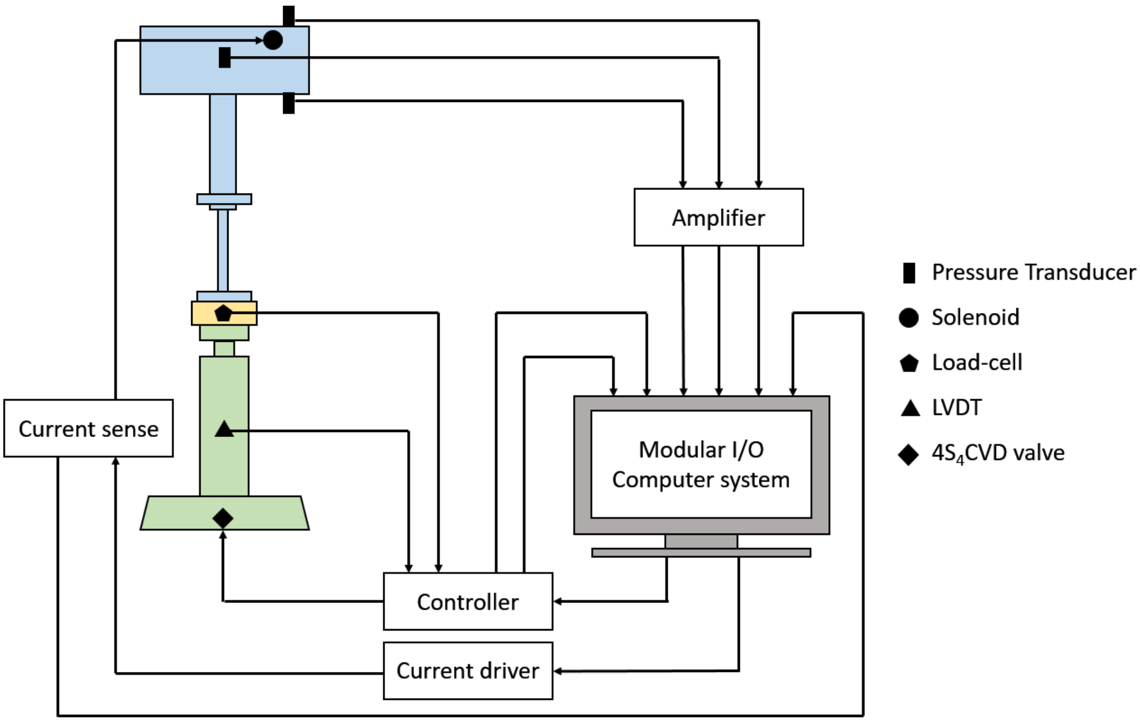

Figure 3: Experimental setup schematic

The force output of the $4S_4CVD$ is a function of the translational input provided by the actuator, as well as the current through the solenoid, which provides the electro-mechanical force actuating the valve. The response time of the valve is therefore influenced by the electric circuit which delivers the current. To characterise the damping and response time of the $4S_4CVD$, a dual output bench power supply with current regulation was combined with a metal-oxide-semiconductor field-effect transistor (MOSFET) switching circuit. With the MOSFET specified to switch within 1ms, the response time is dependent on the power supplies' ability to produce and maintain the current output. The switching circuit also allows for the current through the solenoid to be determined by measuring the amplified voltage across the sensing resistor. Although this current controller is not able to deliver continuously variable current as planned for vehicle implementation, it can provide the constant, step up or step down current signals to characterise the damping and response time of the $4S_4CVD$.

To ensure the current controller had a suitable response time and accuracy, it was investigated by charging and discharging the solenoid valve with a step input and comparing the command signal with the current measured by the current sense circuit indicated in Figure 4. The time it takes for the current to change by 63% from its initial to its final value is referred to as the response time. The extracted charging and discharging response time of the current driver is shown in Figure 5. These results showed response times for charging the solenoid from an initial current of 0A and discharging to a final current of 0A at various step sizes. The results showed satisfactory response times with less than 1.5ms for discharging the solenoid, while charging took 1.5ms to 5.7ms, depending on the current step size. It was estimated that this would be sufficiently faster than the valve dynamics, ensuring the valve response time won't significantly be influenced by the current controller, which was later confirmed through further testing.

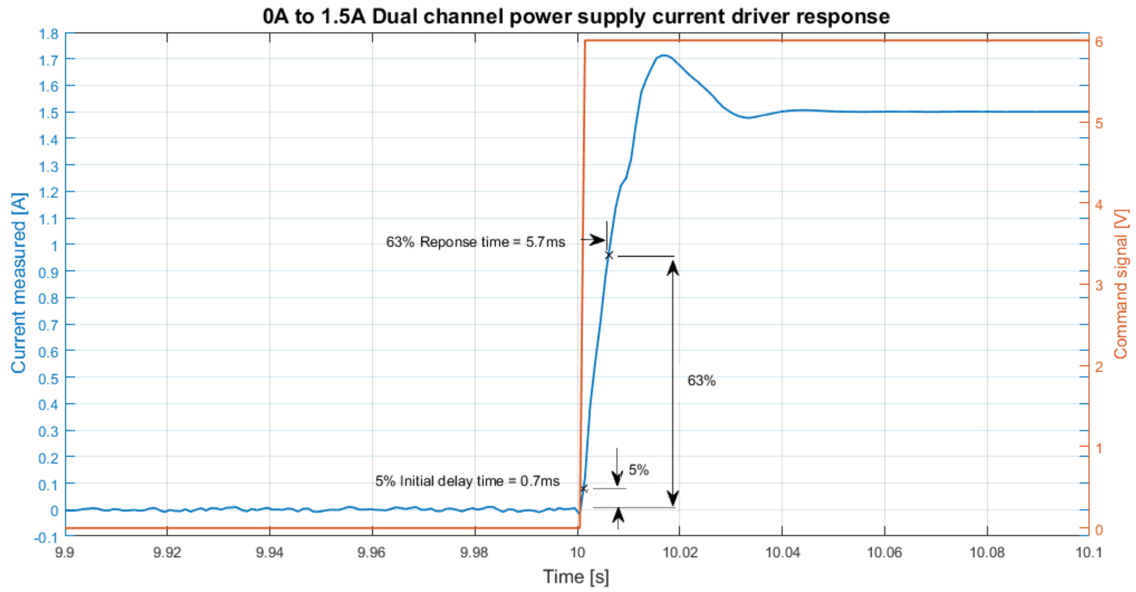

Figure 4: Example current controller response time test results

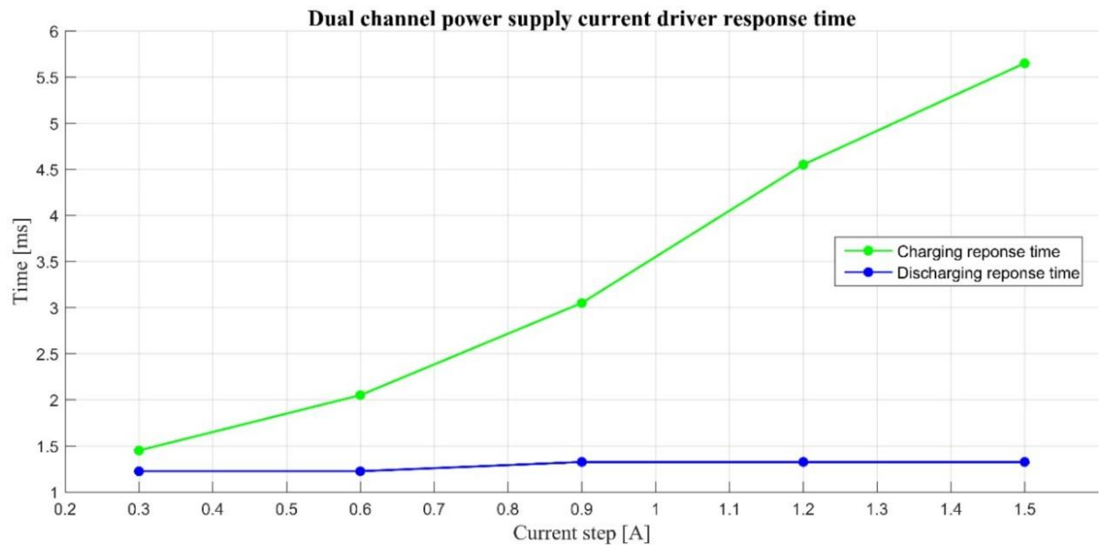

Figure 5: Current controller response time for various current step

3. MODELLING

To characterise the $4S_4CVD$, the suspension underwent extensive experimental testing by subjecting it to various displacement and current inputs, while recording the pressure, force and displacement required for mathematical modelling and validation. In developing a mathematical model, suspension force resisting compression and relative compressive displacement or velocity is considered negative, while extension or rebound is considered positive.

3.1 *Modelling Approach*

The model was initially developed with the one-accumulator testing layout so that it could be validated by comparing predicted force output with the measured results. The force output is directly related to the pressure of the suspension fluid in the strut cylinder. This pressure is determined by a combination of the accumulator pressures, as well as the corresponding pressure drop, ΔP_{valve}, over the valves and channels due to the fluid flow rate. The accumulator pressure depends on the gas volume of the accumulators that changes relative to the strut displacement, while the damping depends on the fluid flow that changes relative to the strut velocity. For the single-accumulator $4S_4CVD$, the force output of the model, $F_{4S_4CVD^*}$ can be described mathematically by:

$$F_{4S_4CVD^*} = -[A \times (\Delta P_{valve} + P_{accu})] + F_f \quad \textbf{(1)}$$

where A is the piston rod area, ΔP_{valve} the pressure drop over the valve, P_{accu} the accumulator pressure and F_f the friction force. This modelling approach and its sub-models can be described by the inputs and outputs indicated in Figure 6. x and $\dot{x}$ is the suspension displacement and velocity respectively, T_{gn} refers to the gas temperature and I the solenoid current command signal. The suspension model ($4S_4CVD$ Matlab-file which comprises of the 3 sub models) can be integrated in the desired vehicle model to conduct vehicle dynamic simulations.

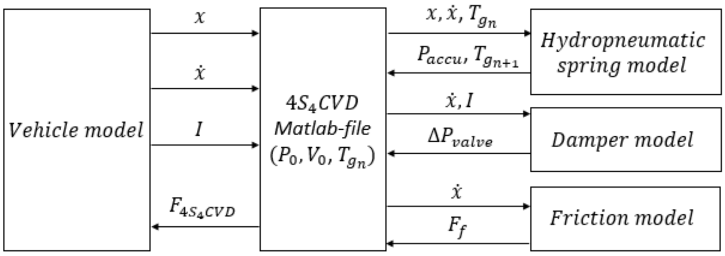

Figure 6: $4S_4CVD$ model layout and interaction

3.2 *Hydropneumatic spring*

To calculate the accumulator pressure, the Benedict-Webb-Rubin (BWR) real gas approach (Otis and Pourmovahed, 1985) was used as in eq. (2). This model calculates the gas pressure based on the specific volume relationship, v, while also accounting for the gas temperature, T_g. R is the universal gas constant while a, A_0, b, B_0, c, C_0, α, γ are all BWR constants specific to Nitrogen.

$$P = \frac{RT_g}{v} + \frac{B_0RT_g - A_0 - \frac{C_0}{T_g^2}}{v^2} + \frac{bRT_g - a}{v^3} + \frac{c\left(1 + \frac{\gamma}{v^2}\right)e^{-\frac{\gamma}{v^2}}}{v^3T_g^2} \quad \textbf{(2)}$$

The BWR real gas approach, combined with the energy equation approach, was proven by Els and Grobbelaar (1993) to accurately predict the spring force in a hydropneumatic suspension system. This approach ensures that the heat transfer between the gas and its environment is taken into account for improved accuracy. Based on convective heat transfer principles, the differential equation as proposed by Otis and Pourmovahed (1985) after some mathematical manipulation can be written as:

$$\dot{T}_g = \frac{T_s - T_g}{\tau} - \frac{\dot{v}}{c_v}\left[\frac{T_g R}{v} + \frac{T_g B_0 R}{v^2} + \frac{2C_0}{T_g^2 v^2} + \frac{T_g b R}{v^3} - \frac{2c}{v^3 T_g^2}\left(1 + \frac{\gamma}{v^2}\right) e^{-\frac{\gamma}{v^2}}\right] \quad \textbf{\textit{(3)}}$$

where c_v is a specific heat constant, T_s the ambient temperature and τ the thermal time constant. The thermal time constant is a measure of the heat transfer coefficient between a gas in a closed container and its surroundings, which can be determined experimentally. Eq. (3) is a first-order differential equation that can be solved to determine the needed gas temperature, T_g. However, the specific heat, c_v first needs to be determined, as given by Otis and Pourmovahed (1985):

$$c_v = c_v^0 + \frac{6}{T_g^3}\left(\frac{C_0}{v} - \frac{c}{\gamma}\right) + \frac{3c}{T_g^3}\left(\frac{2}{\gamma} - \frac{1}{v^2}\right) e^{-\frac{\gamma}{v^2}} \quad \textbf{\textit{(4)}}$$

where the ideal gas specific heat, c_v^0, temperature dependence can accurately be approximated by eq. (5) as given by Jacobsen and Stewart (1973), with N_1 to N_9 and y being constants for Nitrogen:

$$c_v^0 = R\left[\frac{N_1}{T_g^3} + \frac{N_2}{T_g^2} + \frac{N_3}{T_g} + (N_4 - 1) + N_5 T_g + N_6 T_g^2 + N_7 T_g^3 + \frac{N_8 y^2 e^y}{(e^{y}\text{-} - 1)^2}\right] \quad \textbf{\textit{(5)}}$$

To ultimately determine the accumulator gas pressure, eq. (5) and then (4) needs to be calculated, which is then substituted into eq. (3) to determine the changes in gas temperature. Finally, the gas temperature can be derived to calculate the gas pressure in eq. (2). The input to eq. (3) to (5) is the specific gas volume. This changes as the volume of the accumulator changes depending on suspension deflection while the mass of nitrogen gas remains constant. The mass of nitrogen gas that the accumulator was filled with initially is determined by the ideal gas law, described by eq. (6):

$$v = V/m = V/\left(\frac{P_0 V_0}{R T_s}\right) \quad \textbf{\textit{(6)}}$$

To accurately determine the volume of the accumulator, V for a given displacement input, x the compressibility of the oil is taken into account by eq. (7):

$$V = V_0 + xA + \Delta V_{oil} \quad \textbf{\textit{(7)}}$$

where V_0, is the initial charged volume of the accumulator, A the piston area of the suspension and ΔV_{oil}, the volume decrease of the oil due to its compressibility. This is determined based on bulk modulus, β of the oil:

$$\Delta V_{oil} = \left(\frac{\Delta P}{\beta}\right) V_{0,oil} \quad \textbf{\textit{(8)}}$$

ΔP, refers to the difference in filling pressure (atmospheric) and operating pressure, which is equivalent to the current accumulator pressure. $V_{0,oil}$ is the volume of the oil which the unit was filled with.

Lastly, the rate of change of specific gas volume is required in eq. (3). The rate at which the oil volume changes, $\Delta\dot{V}_{oil}$ is assumed to be negligible as the rate of change in pressure is also expected to change gradually between each time step. Thus, the rate of specific volume change of the nitrogen is determined based on the strut velocity, $\dot{x}$:

$$\dot{v} = \dot{x}A/m \quad \textbf{\textit{(9)}}$$

The model therefore solves eq. (2) to (9) at each time step to calculate the gas pressure inside the accumulator required to ultimately determine the force output of the suspension unit as in eq. (1).

3.3 *Controllable damper*

To model the pressure drop across the valve and valve block, a curve fitting method was used based on experimental data. A surface plot of the pressure drop dependant on the input velocity and current was developed, as shown in Figure 7, along with the experimental data points ranging from 0 to 1.2A. Various fit methods were investigated, however, it was found that using Matlab's thin-plate spline method for interpolation achieved the best results. Due to the large pressure drop differences between the 0.9A and the 1.2A setting, some undulations could be noted on the surface plot around -200mm/s, which would not be representative of the actual damping. This could be improved if additional data points were measured and used to refine the model in future.

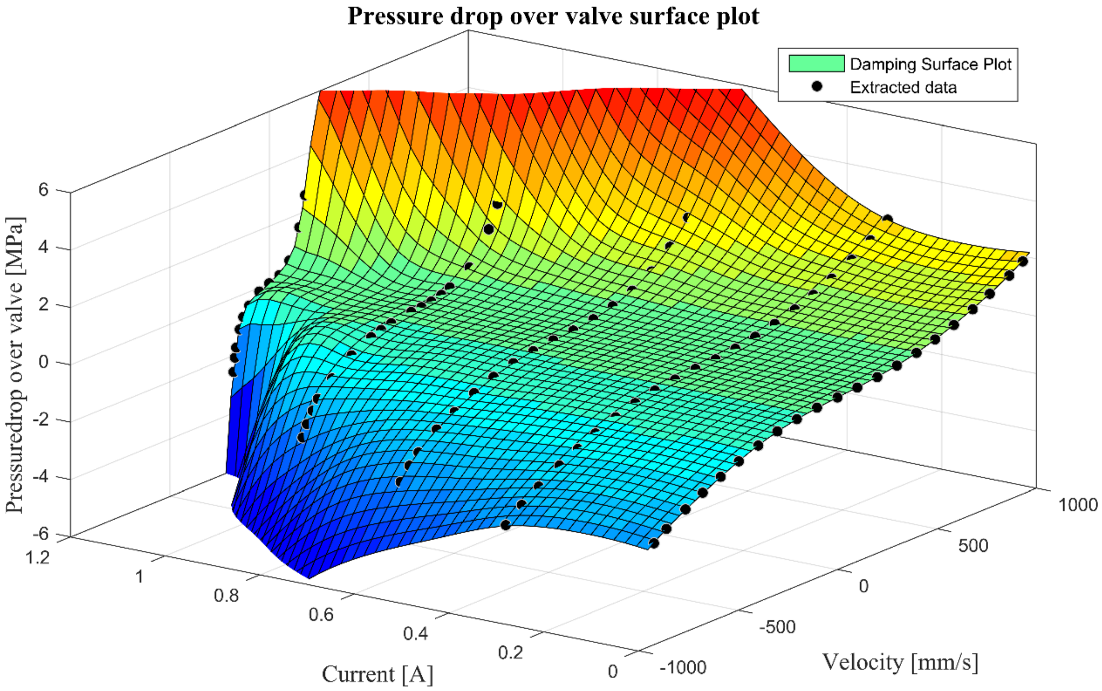

Figure 7: Surface plot of model and data pressure drop over valve

To account for the dynamic behaviour of the valve, the response time is included in the damper model by delaying and controlling the rate of change of the current input to the model. To characterise the response time of the $4S_4CVD$, the suspension was actuated at a specific velocity and then the valve was given a current step input about halfway during the actuation stroke. Figure 8 shows how the response time could be determined based on the solenoid current and pressure drop measured across the valve for a 1.2A current input with 100mm/s actuation. Figure 9 shows the recorded data when the velocity is increased with smaller current steps, which starts to show signs of overshoot of pressure drop due to the actuator not being able to maintain the exact input velocity. For higher velocity inputs as in Figure 10, the measured results become even more unclear and it's not possible to accurately determine the response time.

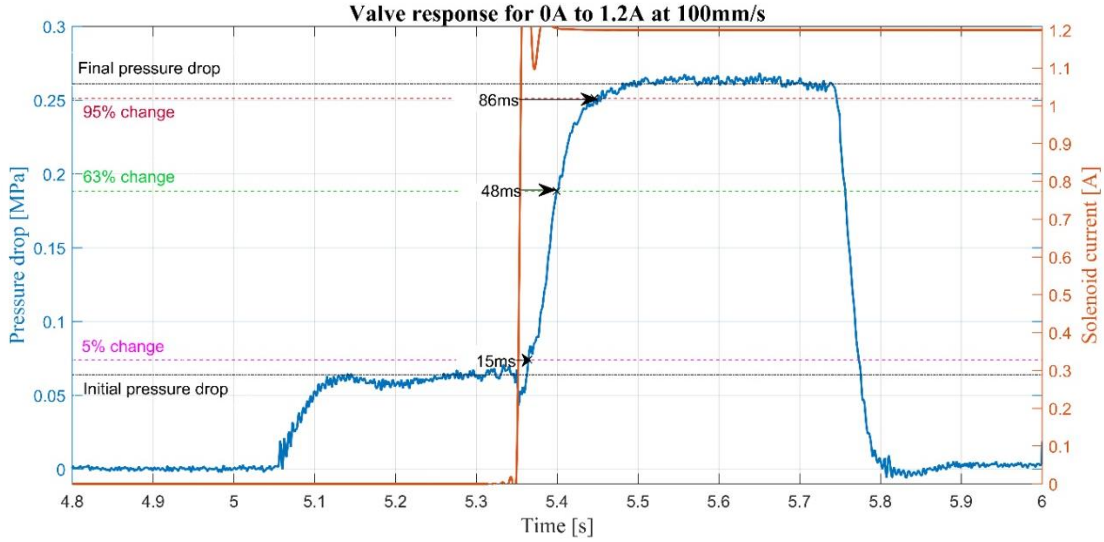

Figure 8: Illustration of extracting valve response time

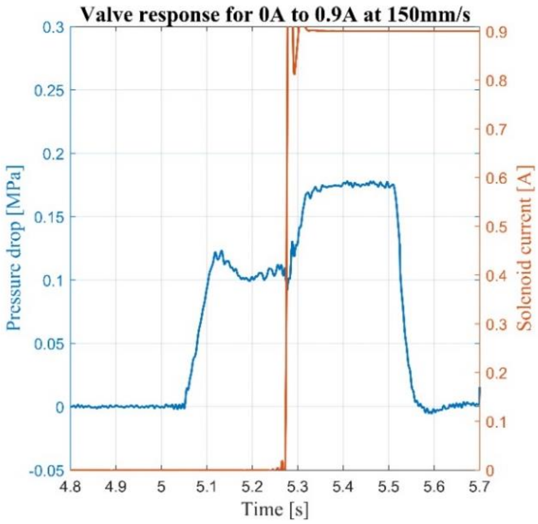

Figure 9: Valve response with overshoot

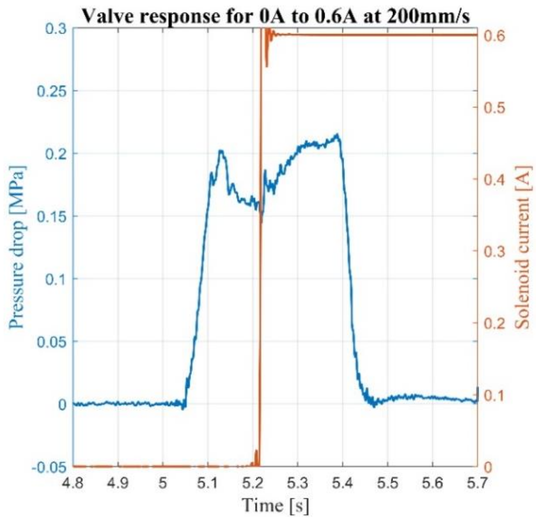

Figure 10: Unclear valve response

Because of the relatively short usable stroke of the $4S_4CVD$ combined with the actuator needing time to stabilise to the desired input velocity, it became difficult to achieve the steady pressure drop before and after switching at higher velocities. The current experimental setup therefore wasn't capable of extracting the full response time profile of the $4S_4CVD$. Figure 11 shows the limited results for various pressure differences between the initial and final pressure drop. It can be noted that closing the valve to the 1.2A state responded under 50ms, while the 0.9A state was faster at about 37ms. Opening from 1.2A and 0.9A to 0A damping state was much faster at under 8ms and 12ms respectively. The response time is therefore dependent on the step size of the current and the change in pressure drop created due to the changing solenoid current. Except in the extreme cases (i.e. 1.2A step which is unlikely unless different spring setting is commanded), the results illustrate that the valve is capable of responding within 40ms. Due to limited data and in order to simplify control a 40ms first order delay was added to the current signal before it reaches the damper model to account for the response time.

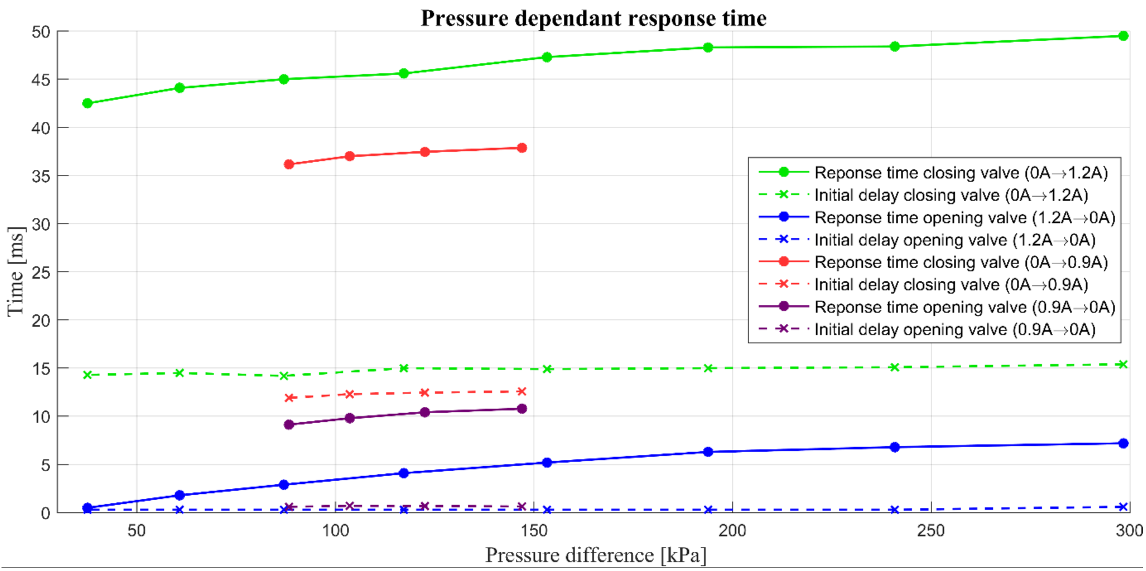

Figure 11: 4S$_4$CVD pressure dependant response time

3.4 *Friction*

Van Den Bergh (2014) showed that the friction force has a significant effect on the simulation results of hydropneumatic suspension systems. However, he concluded that the accuracy gained by using a complex model over a simplified look-up model based on experimental data does not justify the additional computational demand. Therefore, to include the frictional force in the model, the friction force is modelled according to the experimental results. Piecewise cubic Hermite interpolation of the data points was used to calculate the frictional force for a given velocity input. The results indicated that the frictional force remains constant at higher velocities. The resultant model, along with the experimental data used, is presented in Figure 12.

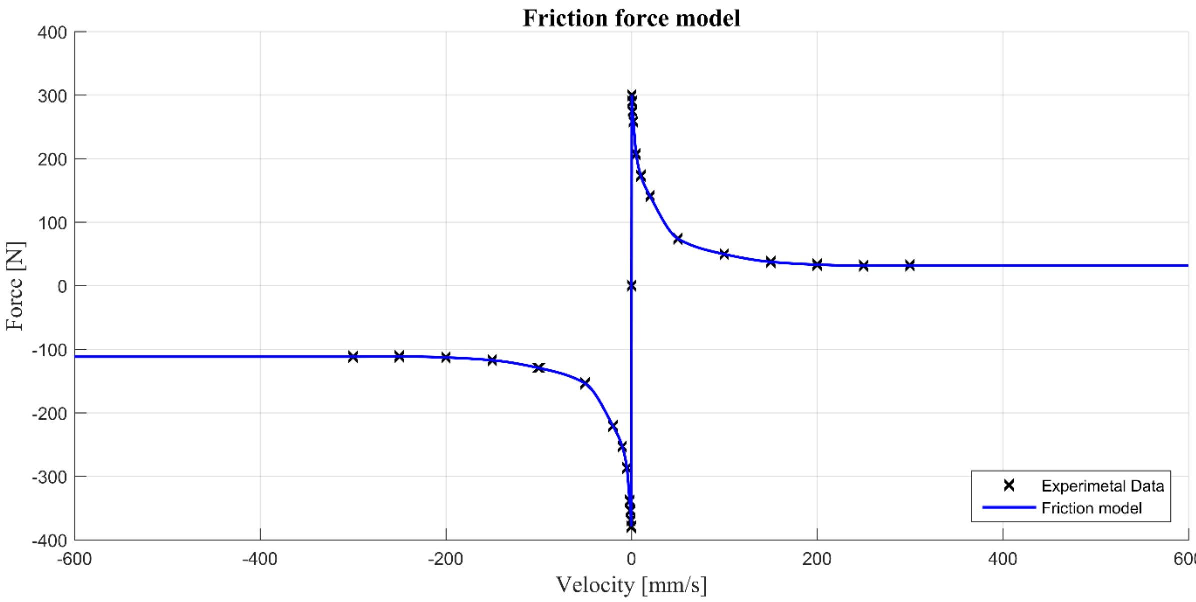

Figure 12: 4S$_4$CVD friction model

4. Validation

To validate the model with the focus on the hydropneumatic spring and friction force, both the model and physical suspension was given the same triangular displacement input, actuated at 1mm/s as shown in Figure 13. The load-cell and accumulator pressure measured is compared to the model-predicted responses as shown in Figure 14. The measured and model-calculated force and pressure correlate well for this input. This proves that the model accurately compensates for the compressibility of the oil, which would otherwise have resulted in an overestimated force output at higher pressures. The hysteresis with regard to heat transfer between the environment and the unit is also accurately included. Higher velocity inputs, however, result in more heat generated. This needs to be investigated to further validate the model in terms of heat transfer. The stability and accuracy of the hydropneumatic spring model is evaluated at higher velocity inputs along with the damping validation as the force output is then not only function of the hydropneumatic spring, but also a damping model. Note that the initial accumulator and suspension fluid volume was estimated based on design parameters which were used to as initial parameters for the model of the $4S_4CVD$. Due to these uncertainties the initial parameters were slightly modified until the best fit was achieved. Tuning of these values can also be justified to account for manufacturing tolerances, deformable accumulator diaphragm or air diffused into the oil. This approach therefore compensates for other compressibility effects that are not included in the model

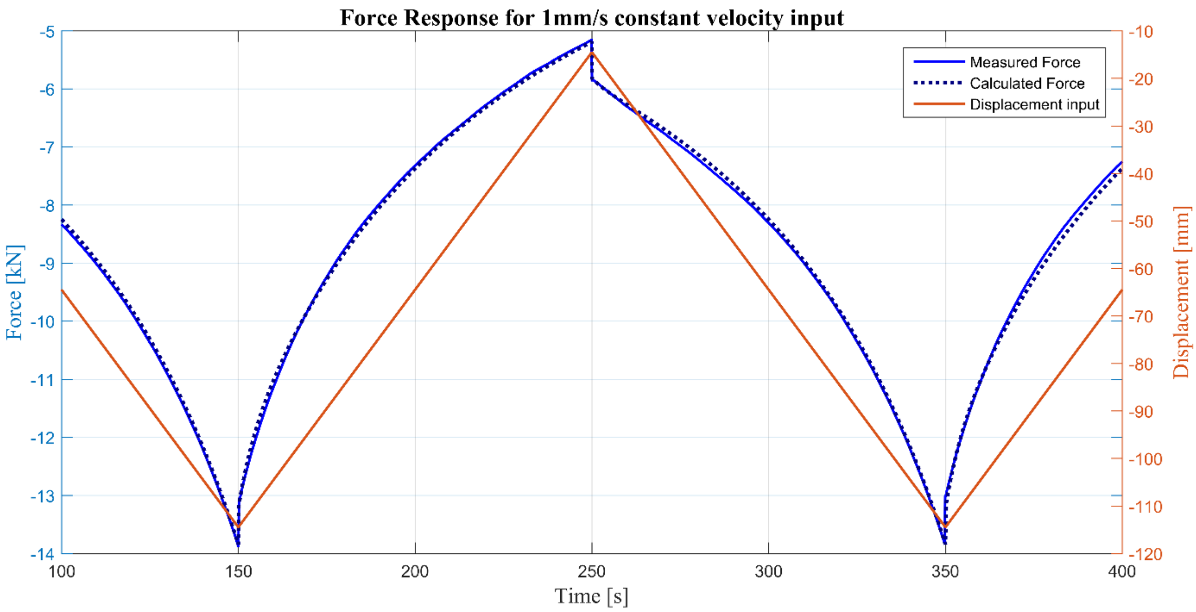

Figure 13: Measured and calculated force response with no damping

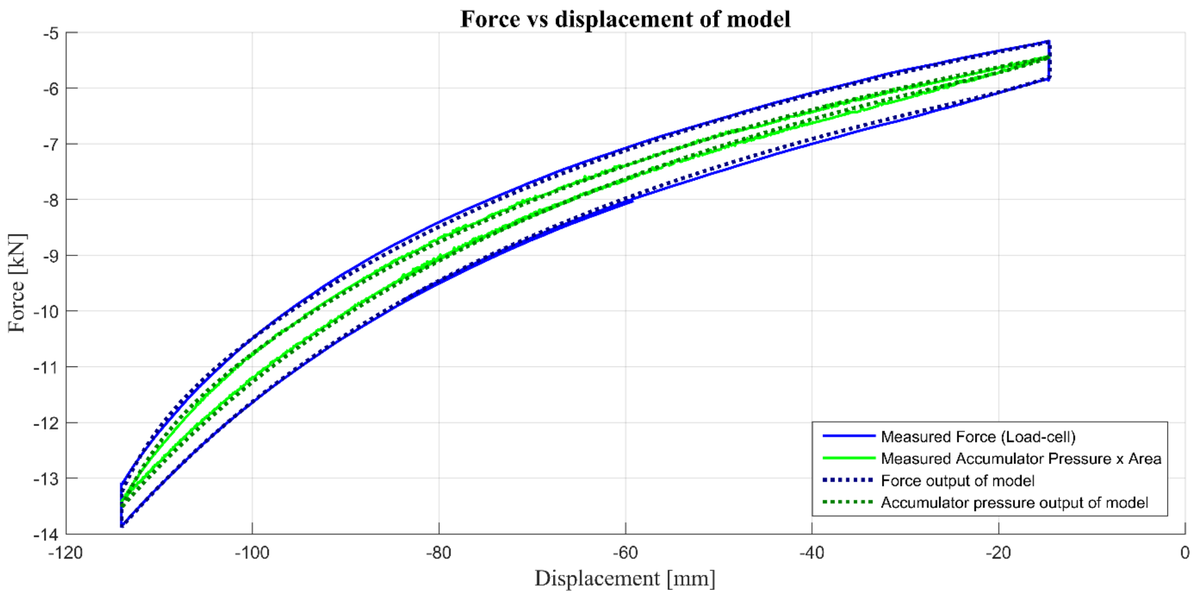

Figure 14: Measured and calculated force versus displacement with no damping

To validate the model with more of a focus on the damping and pressure drop, the response to a triangular displacement input at a higher velocity was investigated. Figure 15 and Figure 16 shows the measured and predicted outputs for an input velocity of 600mm/s combined with a solenoid current of 0.6A. The modelled and measured forces shown in Figure 15 generally correlates well, while the pressures shown in Figure 16 correlates even better. The initial force offset can be ascribed to the residual force due to stick slip friction, which disappears as the actuator displaces the strut. Some force discrepancies can be noted when the input velocity abruptly changes (high acceleration), however, the model returns to the measured force within 20ms. This can be attributed to not taking into account the inertial properties of the piston rod, bearing and mounting that has mass of more than 10kg. In full-vehicle simulation this should be accounted for by combining the mass of the piston and mounting with the unsprung mass so that the dynamic effects are taken into account by the multibody vehicle dynamics model. Since the damping model was developed using constant velocity inputs, there were some concern that it would not be capable of accurately calculating the pressure drop in dynamic situations where the velocity changes abruptly. However, as the calculated pressure responses shown in Figure 16 correlate so well, it can be concluded that the model accurately predicts the pressure drop even in these dynamic conditions (i.e. the inertial effects are negligible).

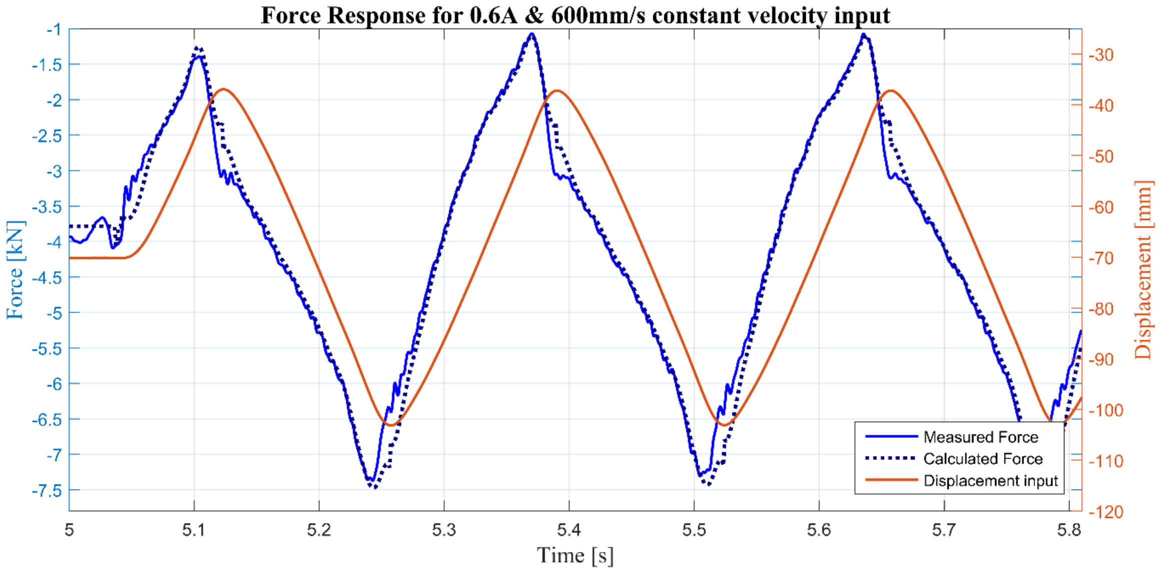

Figure 15: Measured and calculated force response with 0.6A damping

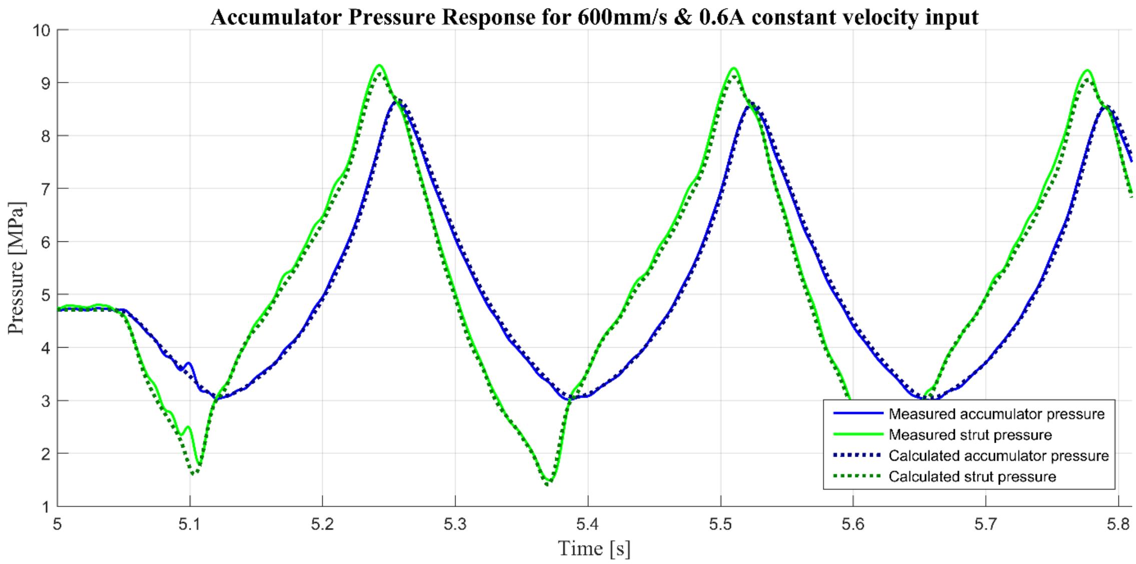

Figure 16: Measured and calculated pressure response with 0.6A damping

For further validation, a dynamic input based on an artificially generated class-D road, based on the ISO 8608 standard (International Organization for Standardization, 1995) was used. The generated road had a total displacement of 180mm, which exceeds the stroke length of the $4S_4CVD$ used during testing. The peak input displacement was therefore reduced to 80mm by scaling the total displacement input by a factor of 0.44, i.e. it is not a true representation of a class D road anymore. A constant current to the solenoid valve was applied based on the maximum velocity of the input to ensure moderate damping, while reducing the risk of damaging the suspension unit due to excessive damping forces. This also reduces complexity and remove ambiguity in the results. The scaled road profile in the spatial domain is converted to the time domain, based on the speed a vehicle would drive over it. A vehicle speed was determined based on the desired velocity that correlates to the chosen solenoid current. For a 0.9A solenoid current, a vehicle speed of 20km/h was selected as it results in a maximum input velocity of 400mm/s. This is within the parameters used during the characterisation tests and would generate adequate damping while not producing excessive damping forces.

An extract of the measured and calculated force, along with the displacement input, are presented in Figure 17. The sudden "steps" or discontinuities in the force response are caused by friction in the system. The suspension is fixed while forcing it with a specific displacement input and as the direction of the input velocity changes the direction of the frictional force changes, resulting in a discontinuity. In reality the actual actuation of the suspension would be different due to the filtering effects of the tyre and the vehicle body being able to translate vertically, however, this can still be used to validate the model. Overall, the model-calculated force output correlates well with the measured force. The largest offset can be noted at large displacements where the force predicted by the model is marginally higher than what was measured, as can be seen at 5.3 seconds (indicated by the ellipse in the figure). This discrepancy could be due to the pressure dependence of the frictional force. At 5.3 seconds the piston is extended, resulting in a positive friction force. Because the pressure is higher than what was used to develop the friction model, the frictional force is therefore larger than what the model calculates which would explain the slight offset.

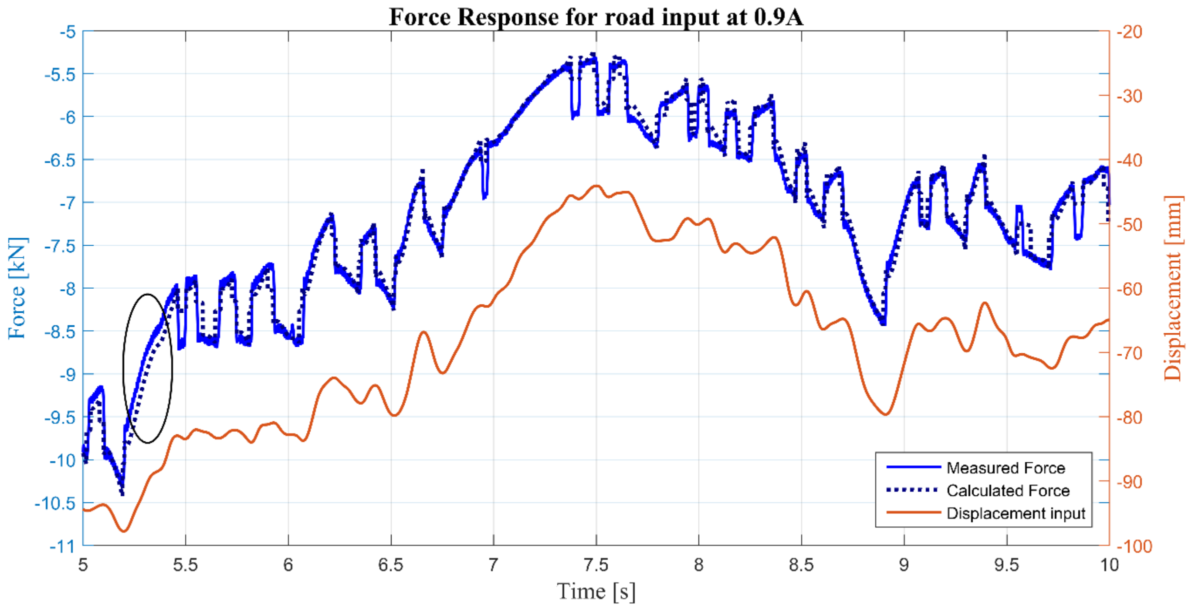

Figure 17: Measured and calculated force for an artificial road input

5. FULL $4S_4CVD$ MODEL

After validating the single-accumulator and valve model according to experimental data, the model was extended to the full, two-accumulator model of the $4S_4CVD$ intended for vehicle implementation. Experimental testing of the full, two-accumulator $4S_4CVD$ did, however, not form part of this study, and can therefore not be validated. However Theron and Els (2007) as well as Heymans et al. (2016) developed a hydropneumatic suspension model that similarly relied on determining the flow split between two accumulators as with the $4S_4$. Good correlation between the predicted force output and measured experimental results of the $4S_4$ demonstrates that the incorporation of flow-split modelling is a suitable and accurate strategy.

5.1 *Flow split calculation*

The full $4S_4CVD$ model consequently consists of the validated hydropneumatic spring, damping and friction models. The input to the hydropneumatic spring and damping model is determined by the fraction of fluid flowing along each respective path, as indicated in Figure 18. The fluid flow caused by displacement of the piston rod, Q_3, and the equivalent flow split can be described by eq.(10):

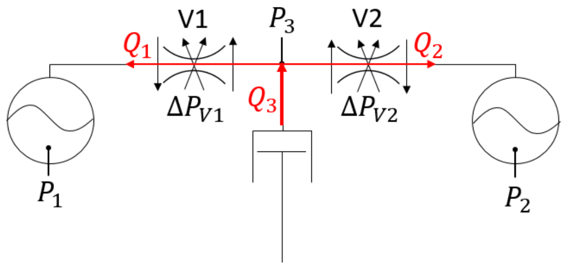

Figure 18: Fluid flow model

$$Q_3 = A_{piston}\dot{x} = Q_1 + Q_2$$
$$Q_3 = \left[\left(Q_{frac} \times Q_3\right) + \left(1 - Q_f\right)Q_3\right] \tag{10}$$

Q_1 and Q_2 is the flow rate through the valve to accumulators 1 and 2 respectively. Q_{frac} is the fluid-flow fraction where 1 would mean that all the fluid flows to accumulator 1 and 0 that all of it goes to accumulator 2. The correct flow split will result in the system being in equilibrium, so that there is no pressure differential. For the system to be in equilibrium, the accumulator pressure and pressure drop over the valve needs to equal the strut pressure as described by eq. (11). This equation can be rewritten in terms of both the accumulator pressure and pressure drop as in eq. (12). The flow split is then calculated by using Matlab's *fminbnd.m* function, a minimiser function that iteratively changes the flow split (starting at 0.5, limited between 0 and 1) until it finds the minimum for eq. (12). The maximum allowed iterations for the minimiser function was set at 500 and the threshold or tolerance for allowed minimum set at 10Pa.

$$P_3 = P_1 + \Delta P_{V1} = P_2 + \Delta P_{V2} \tag{11}$$

$$(P_1 + \Delta P_{V1}) - (P_2 + \Delta P_{V2}) \approx 0 \tag{12}$$

Accumulator pressures, P_1 and P_2, are calculated with the hydropneumatic spring model and the pressure drop over valves 1 and 2, ΔP_{V1} and ΔP_{V2}, are calculated with the damping model. For a compressive input, increasing the flow fraction would therefore increase accumulator 1 pressure, P_1, as more fluid flows to the accumulator decreasing the volume. The pressure drop over valve 1, ΔP_{V1}, would also increase due to the increased flow. However, the pressure of accumulator 2, P_2, would decrease and the pressure drop created over valve 2, ΔP_{V2}, would also be lower. The opposite would happen if the fraction were to be decreased. The minimiser function determines the split resulting in equilibrium for each time step before the force output can finally be determined by eq. (13):

$$F_{4S_4CVD} = (A \times P_3) + F_f \tag{13}$$

5.2 *Inter-accumulator flow error*

After analysing the output of the model, it was found that the model produces a residual pressure offset between the two accumulators after a given input. Figure 19 illustrates this in the pressure response solved at 1kHz for an artificial triangular displacement, 400mm/s constant velocity input with 0.9A current supplied to both valves, but with different accumulator volumes. The pressure differential between the two accumulators should be negligible after 1.1s, since there is no velocity input to create a pressure drop over the valves. After further investigation it was found that this offset is due to the model not being capable of accurately predicting the force output when given an artificial triangular displacement input where the velocity changes from 400 to 0mm/s in 1 time step. At 400mm/s there is fluid flow and a pressure differential in accumulators due to the different pressure drop over the valves. In the following time step the input could change to 0mm/s which equates to no fluid flow calculated in the model. This results in zero pressure drop over the valves, but there is still the residual pressure differential between the accumulators carried over from previous solve step, but now no flow to allow recalculation to satisfy equilibrium. This translates into an inaccurate prediction of the force output, which is clear when checking if the system satisfies equilibrium as defined in eq. (11).

To solve this problem, a strategy was incorporated that allows flow between the accumulators when the piston velocity becomes low and equilibrium is not satisfied after the flow split has been calculated. After the appropriate flow split is calculated and the equilibrium error is more than 10Pa, a minimiser function is again used to find equilibrium iteratively by changing the amount of fluid flow between the accumulators, Q_{2to1}. The flow to each accumulator can then be defined by eq. (14).

$$\begin{aligned} Q_1 &= Q_1 + Q_{2to1} \\ Q_2 &= Q_2 - Q_{2to1} \end{aligned} \tag{14}$$

This flow is used to calculate the accumulator pressures and pressure drops within the respective models, which is then used to assess equilibrium with eq. (11). Figure 20 shows the pressure response of the model that includes this inter-accumulator flow strategy. After 1.1s the model now allows fluid flow from accumulator 1 to accumulator 2, even though there is no fluid flow caused by the piston displacement. The corresponding equilibrium error is now less than 0.1Pa. Evidently, incorporating this inter-accumulator flow strategy greatly increases the accuracy of the full $4S_4$CVD model.

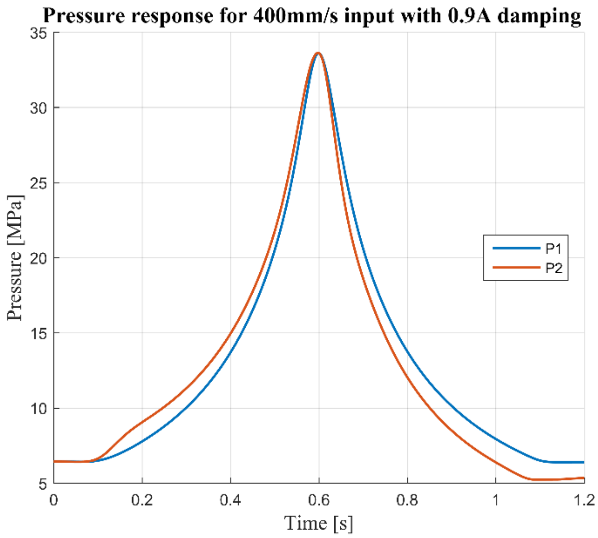

Figure 19: Full model response error without inter-accumulator flow

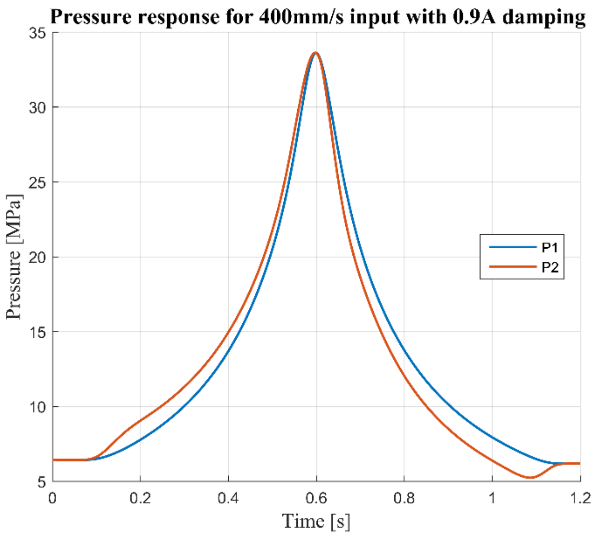

Figure 20: Full model response with inter-accumulator flow

5.3 *Full $4S_4$CVD characteristics*

An optimisation study by Uys et al. (2007) determined that a total accumulator volume of $0.1l$ and $0.5l$ for the $4S_4$ provided optimum ride comfort and handling performance. A similar study is required to investigate which accumulator volumes for the $4S_4$CVD would be optimal. As a first estimate, the accumulator volumes and charge pressure of the full $4S_4$CVD model is selected to produce similar spring characteristics as the already optimised $4S_4$. After exploring different accumulator volumes and charge pressures with the full $4S_4$CVD model, it was found that a total volume of $0.27l$ at a charged pressure of 3.65MPa provides a similar soft spring characteristic, as shown in Figure 21. Any combination of the two accumulator sizes could essentially be used to make up the combined volume. Having two different size volumes does allow an additional spring characteristic. However, to achieve a similar hard spring characteristic of the $4S_4$ an accumulator volume of $0.145l$ is required, which requires the remaining accumulator volume to be $0.125l$ to achieve the desired total volume. This effectively eliminates a third spring setting as these volumes produce similar spring characteristics.

Alternatively, volumes of $0.16l$ and $0.11l$ can be used, which produced a characteristic that was both lower and higher than the hard $4S_4$ setting, as shown in Figure 21. It should however be noted that Els (2006) stated the hard spring of $4S_4$ to be sufficiently high. Therefore, it might be better to increase the total volume, which decrease the soft spring of the $4S_4$CVD, but allows more freedom in selecting different accumulator volume combinations. Future research initiatives which focus on finding optimal volumes should address this problem.

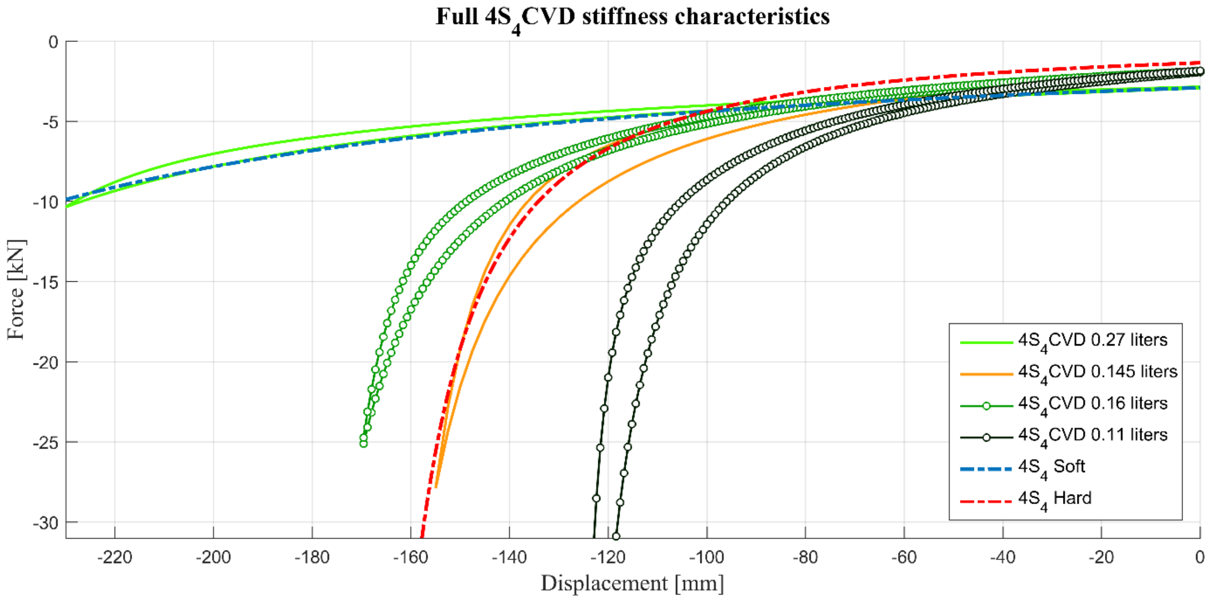

Figure 21: Possible spring characteristics for the two-accumulator 4S4CVD

The force output of the full $4S_4$CVD model is essentially always a combination of a spring, friction and a damping force. The damping or force versus velocity characteristics can however, selectively be extracted by determining them from the total pressure drop over the valves as calculated by the model. Figure 22 shows the possible damping characteristics of the $4S_4$CVD, along with the $4S_4$ damping characteristics and the stock or baseline damper for comparison. The characteristics were determined using a 100mm sine wave as input, with the frequency chosen to produce a reasonable damping effect. The soft spring allows fluid to flow to both accumulators, while the stiff spring blocks flow to one accumulator by supplying a 1.5A current. To simplify the process, it was assumed that there is no leakage past the valve, since tests indicated it to be negligible. In the case of the soft spring, both valves were provided with the same current. When flow is allowed to both accumulators, the flow rate through each valve is reduced, which consequently reduces the damping. With the stiff spring, all the fluid is forced through one valve and the damping effect is therefore larger. The $4S_4$CVD would thus be capable of producing any damping characteristic from the lower 0A damping limit (when the fluid flow to one accumulator is blocked) up to and past 1.2A damping, until effectively blocking all flow.

From Figure 22 it is evident that the $4S_4$CVD is capable of producing much lower damping than the baseline and $4S_4$. Els (2006) stated that the $4S_4$ damping should be 50% less for significant ride comfort improvement. When comparing these characteristics, it could be concluded that the $4S_4$CVD soft spring is capable of producing around four times less damping than the soft $4S_4$. Based on this, the $4S_4$CVD would therefore already be capable of providing better ride performance. When considering how the $4S_4$CVD would affect the handling capabilities, the high damping (1.2A damping) can be compared to the $4S_4$ hard or handling setting. In Figure 22 it is evident that even with the stiff $4S_4$CVD setting it provides extremely low damping at velocities below 150mm/s. Although it is possible to increase the damping at low velocities by further increasing the current supplied to the solenoid valve, this would then have a knock-on effect of then causing severe damping (effective lock-up) at velocities below 200mm/s. It is expected that this will be detrimental to the handling capabilities of the vehicle. This problem arises from using flow control valves which causes an exponential increase in damping instead of a more linear increase as with the $4S_4$. Therefore, although the $4S_4$CVD would result in increased ride comfort, it would decrease handling due to negligible low speed damping.

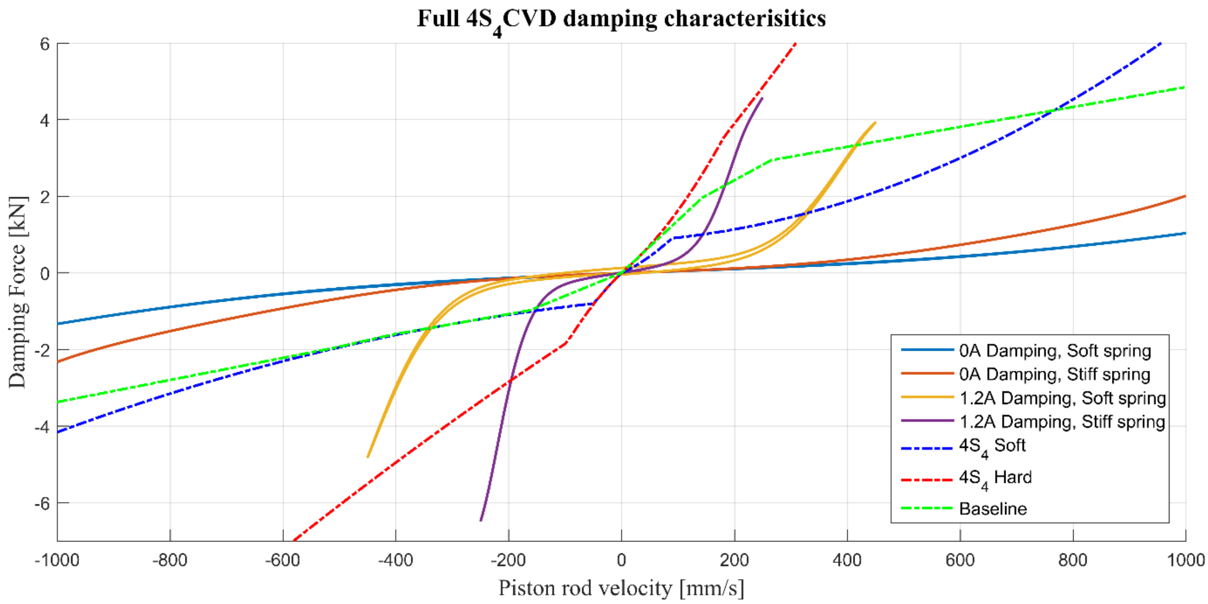

Figure 22: Possible damping characteristics for the two-accumulator 4S4CVD

It was found that the single accumulator and valve model of the 4S4CVD successfully predicts the force output of the suspension across a range of operation and could be validated according to experimental results. This model was extended to the full, two accumulator and two valve model by incorporating proven flow split strategies using Matlab's *fminbnd.m* function to ensure equilibrium, however, this comes at a relatively large computational cost. Even with a fairly capable 4th generation 3.2GHz processor, the model takes roughly 27ms per time step to solve, which translates to less than 40Hz for real-time simulation).

The accuracy of the model could degrade if the sampling frequency is not kept sufficiently high. A high sampling rate is especially critical when the model includes a control strategy as it adds additional delay in the response. It is possible that a control strategy, which depends on solving the model real-time, would require a simplified or optimised suspension model to implement and test experimentally. This would depend, and form part of future investigations.

6. Conclusion

The $4S_4$CVD suspension was successfully characterised by actuating a single accumulator version of the suspension on a test bench to ensure that the valve dynamics could accurately be captured without having to account for two flow paths. The spring and damping characteristics, friction and response time of the $4S_4$CVD were extracted by subjecting the unit to various inputs while controlling the valve. The suspension unit was capable of producing continuously variable damping as well as discrete spring characteristics based on the current supplied to the solenoid valve.

The $4S_4$CVD therefore successfully incorporated continuously variable damping in the proven vehicle-implemented $4S_4$. Furthermore, the test results indicated that the $4S_4$CVD successfully reduced the lower damping limit by up to 50% compared to the $4S_4$. This is expected to yield improved ride comfort due to increased small bump compliance. However, it was noted that the suspension provides very low damping at the lower velocities despite the solenoid valve in a high damping setting. Although it is possible to increase the damping at low velocities by further increasing the current supplied to the solenoid valve, this would then have a knock-on effect of causing extreme damping when the velocity increases slightly. This highly exponential damping curve could be detrimental to the handling performance. Further simulation based investigations are required to quantify the how these aspects would affect ride and handling performance, therefore, determining whether the $4S_4$CVD is suitable successor to the $4S_4$.

The response time was found to be dependent on the magnitude of the input current step and the change in pressure drop the actuation of the valve will result in. Except for the extreme cases, the results showed that the valve is capable of responding within 40ms. The dynamic performance of the test setup directly influences the accuracy and range in which the response time can be determined. Without being able to precisely control the pressure drop and flow in a high bandwidth range across the entire range of operation, it was not possible to extract the full pressure and current dependant response time profile of the suspension. To accurately determine the response time for the suspension with a continuously variable valve, a more controlled environment would be required to produce the dynamic states. Alternatively, a detailed model of the actuator is required in order to separate the actuator dynamics from the suspension or valve dynamics.

A mathematical model of the single accumulator version of the suspension was developed and validated according to experimental data. This model was successfully extended to the full, two accumulator and valve version of the $4S_4$CVD by employing a flow split strategy which can be combined with a vehicle model to conduct simulation based investigations. Although such a strategy has been validated on other hydropneumatic suspension, experimental testing of the full unit is required to confirm this.

The development of the $4S_4$CVD model allows future research initiatives to investigate its ride and handling performance combined with various control strategies and accumulator volumes in simulation. Future work should focus on conducting quarter car and full vehicle simulations to justify further development or vehicle implementation.

7. References

British Standards Institution. 1987.*British Standard Guide to Measurement and Evaluation of Human Exposure to Whole Body Mechanical Vibration and Repeated Shock*, BS 6841.

Els, P. S. 2006. *The Ride Comfort vs. Handling Compromise for Off-Road Vehicles*, PhD Thesis, [Online]. Availible: https://repository.up.ac.za/handle/2263/26302 [Accessed 10 July 2017], University of Pretoria, Pretoria, South Africa.

Els, P. S. & Grobbelaar, B. 1993. *Investigation of the Time-and Temperature Dependency of Hydro-Pneumatic Suspension Systems*. SAE Technical Paper Series no. 930265, pp. 55-65.

Heymans, G. S., Grobler, J. F. & Els, P. S. 2016. *Physics Based Modelling of a Magneto-Rheological Equipped Hydro-Pneumatic Semi-Active Suspension System*. Procedings of ASME 2016 International Design Engineering Technical Conferences and Computers and Information in Engineering Conference, Charlotte, North Carolina. August 21-24, 2016, American Society of Mechanical Engineers.

Hydraforce. 2013. *Electro-Proportional Valves* [Online]. Available: http://hydraforce.com/Proport/Prop_html/2-602-1_ZL70-30/2-602-1_ZL70-30.htm#view9 [Accessed 11 July 2017].

International Organization for Standardization. 1995.*International Standard ISO 8608: Mechanical vibration – Road surface profiles – Reporting of measured data*, ISO 3888-1:1999(E).

Jacobsen, R. T. & Stewart, R. B. 1973. *Thermodynamic properties of nitrogen including liquid and vapor phases from 63K to 2000K with pressures to 10,000 bar*. Journal of Physical and Chemical Reference Data, Vol. 2, pp. 757-922.

Otis, D. & Pourmovahed, A. 1985. *An algorithm for computing nonflow gas processes in gas springs and hydropneumatic accumulators*. Journal of dynamic systems, measurement, and control, Vol. 107, pp. 93-96.

Theron, N. J. & Els, P. S. 2007. *Modelling of a semi-active hydropneumatic spring-damper unit*. International Journal of Vehicle Design, Vol. 45, pp. 501-521.

Van Den Bergh, J.-S. 2014. *Effects of friction and gas modelling on vehicle dynamics simulation*, Unpublished M.Eng Masters, , University of Pretoria, Pretoria, South Africa.

Uys, P. E., Els, P. S. & Thoresson, M. J. 2007. *Suspension settings for optimal ride comfort of off-road vehicles travelling on roads with different roughness and speeds*. Journal of Terramechanics, Vol. 44, pp. 163-175.